

**NPL REPORT  
DEPC-MPE 020**

**Piston dilatometry applied to  
aluminium and nickel alloys**

**R Morrell and R F Brooks**

**NOT RESTRICTED**

JULY 2005



The DTI drives our ambition of 'prosperity for all' by working to create the best environment for business success in the UK. We help people and companies become more productive by promoting enterprise, innovation and creativity.

We champion UK business at home and abroad. We invest heavily in world-class science and technology. We protect the rights of working people and consumers. And we stand up for fair and open markets in the UK, Europe and the world.

The National Physical Laboratory is operated on behalf of the DTI by NPL Management Limited, a wholly owned subsidiary of Serco Group plc

## **PISTON DILATOMETRY APPLIED TO ALUMINIUM AND NICKEL ALLOYS**

R Morrell and R F Brooks  
Division of Engineering and Process Control

### **ABSTRACT**

The use of piston dilatometry is described for the measurement of the melting behaviour for metals and alloys. In this technique, a cylindrical sample of the test alloy is held between ceramic pistons within a ceramic cylinder, and treated as a thermal expansion test-piece. The technique has been applied to a series of Al-Si alloys, with a good match being found between theoretical and experimental liquidus temperatures, widths of solid/liquid phase region (so-called 'mushy' zone), and liquid phase volumetric expansion coefficients. The technique has also been used successfully on a variety of other alloys, including nickel-base superalloys. In some cases, the technique fails because of reactions between the ceramic and metal, or because of leakage of molten metal down the narrow gap between piston and containing cylinder wall.

© Crown copyright 2005  
Reproduced with the permission of the Controller of HMSO  
and Queen's Printer for Scotland

ISSN 1744-0262

National Physical Laboratory  
Hampton Road, Teddington, Middlesex, TW11 0LW

Extracts from this report may be reproduced provided the source is acknowledged and the extract is not taken out of context.

We gratefully acknowledge the financial support of the UK Department of  
Trade and Industry (National Measurement System Policy Unit)

Approved on behalf of the Managing Director, NPL,  
by Dr M G Gee, Knowledge Leader, Materials Performance Team  
authorised by Director, Engineering and Process Control Division

## CONTENTS

<b>1</b>	<b>INTRODUCTION.....</b>	<b>5</b>
<b>2</b>	<b>TEST MATERIALS .....</b>	<b>5</b>
<b>3.</b>	<b>MEASUREMENT METHODS .....</b>	<b>6</b>
3.1	Density.....	6
3.2	Mechanical dilatometry .....	6
3.3	Piston dilatometry .....	7
<b>4.</b>	<b>RESULTS .....</b>	<b>9</b>
4.1	Nickel alloys, Studio programme .....	9
4.2	Aluminium alloys .....	10
4.3	Miscellaneous alloys.....	15
<b>5</b>	<b>DISCUSSION .....</b>	<b>17</b>
<b>6.</b>	<b>CONCLUSIONS .....</b>	<b>19</b>
	<b>ACKNOWLEDGEMENTS.....</b>	<b>19</b>
	<b>REFERENCES.....</b>	<b>19</b>



## 1 INTRODUCTION

Understanding the melting behaviour of metal alloys is crucial to the ability of the casting industry to predict performance in casting operations. Data are needed for calculation programmes for the prediction of required mould dimensions, and for heat transfer during cooling. While progress is being made in theoretical estimations of true melting behaviour of complex alloys in terms of density, solidus and liquidus, experimental techniques remain difficult, and direct measurements are prone to experimental errors, as the scatter of literature data shows [1].

A technique for determining melting behaviour and recording mush and liquid density that was examined in an earlier DTI programme, IMP5, is that of piston dilatometry [1]. In this technique, a ceramic piston and cylinder set is used to provide an enclosed defined volume within which the metal melts, and the volume changes are translated into piston movement which can be recorded by a mechanical dilatometer. A full discussion of the technique appears in NPL report CMMT (A) 106 [2].

In the present report, three further measurement exercises are reported:

1. Measurements on a series of nickel alloys, made as part of an NPL Studio Project;
2. Measurements on a series of aluminium alloys, comparing experimental results with theoretical predictions;
3. Measurements on a series of various high-temperature alloys, including 316L stainless steel and a copper-nickel alloy.

## 2 TEST MATERIALS

Tables 1-3 list the test materials together with analysed (Table 1), nominal (Table 2) or typical (Table 3) compositions.

**Table 1: Test materials – Studio project\***

NPL Code	Material code	Compositional details, wt%
PGK	CM186LC	Ni, 6Cr, 9Co, 0.5Mo, 8W, 3Ta, 5.7Al, 0.7Ti, 1.4Hf, 3Re
PGZ	CMSX10	Ni, 2.3Cr, 3.4Co, 0.41Mo, 5.6W, 8.3Ta, 5.78Al, 0.32Ti, 6.4Re +minor
PHC	René 80	Ni, 14Cr, 9.5Co, 4Mo, 4W, 3Al, 5Ti, + minor
PGA	IN738LC	Ni 16Cr, 8.5Co, 1.7Mo, 2.6W, 1.7Ta, 3.4Al, 3.4Ti, 0.01B, 0.9Nb

\* Supplied by Howmet Ltd, Cannon-Muskegon Inc, and Chromalloy Inc.

**Table 2: Test materials – Aluminium and aluminium alloys**

NPL Code	Material code	Source
-	Pure Al	Johnson Matthey Grade 1
PHP	Al 5Si	Hydro Aluminium Deutschland GmbH (formerly VAW Aluminium AG,), Bonn, Germany
PHR	Al 7Si	
PHS	Al 9Si	
PHT	Al 12Si	
PHU	Al 5Si 0.3 Mg	
PHW	Al 7Si 0.3 Mg	
PHX	Al 9Si 0.3Mg	
PHY	Al 12Si 0.3 Mg	

**Table 3: Test materials – Miscellaneous alloys**

NPL Code	Material code	Compositional details
-	Waspalloy	Ni, 18.0-21.0Cr, 12.0-15.0Co, 3.5-5.0Mo, 1.0-1.5Al, 2.60-3.25Ti, <0.75Si, <2.0Fe, 0.02-0.12Zr, + minor (typical)
PHJ	Cu-Ni*	Cu, 31.5Ni, 1.9 Cr + minor
-	316L Stainless steel**	Fe, <0.03%C, 16-18.5Cr, 10-14Ni, 2-3Mo, <2 Mn, <1 Si, <0.045P, <0.03S

\* Supplied via Meighs Ltd, Sheffield

\*\* Supplied by RS Components Ltd

### 3. MEASUREMENT METHODS

#### 3.1 Density

Room-temperature density measurements were made on regular cylinders of material of volume about 1000 mm<sup>3</sup> using the Archimedes immersion technique on a Mettler electronic balance reading to 10<sup>-5</sup> g. Precautions were taken to minimise the risk of trapping bubbles by cleaning the test-pieces in dilute Teepol solution, and using two drops of this solution in the demineralised water used for the suspension medium. At least three measurements were made on each test sample. The results were consistent to typically  $\pm 0.001 \text{ Mg m}^{-3}$ . The limitations of the technique being the inability to control the liquid level rise up the suspension wire when the sample was placed on the immersed holder.

#### 3.2 Mechanical dilatometry

The specimens were tested in a modified Linseis dilatometer. The instrument operates in the horizontal mode with specially constructed alumina apparatus comprising a tube with an end flat against which the test-piece is pushed by an alumina push-rod. The push-rod transmits the changes in length to a linear displacement transducer as the test-piece is heated and cooled. The temperature of the test-piece is measured using a contacting type R thermocouple, and the



outputs of the thermocouple and the transducer are recorded at 2-min. intervals on a data logger for later analysis.

The instrument is calibrated in the following manner. The alumina test-piece holder is removed, and replaced by a drum micrometer which is used to move the push-rod prescribed amounts. In this way the absolute sensitivity of the transducer may be determined. The apparatus is reassembled and run over the required temperature range with an alumina test-piece of the same material as the push-rod, and any shift of the baseline output, corresponding to differential temperature distributions in the specimen support and push-rod, is determined. This is used to correct the output from testing an unknown. The correction for the expansion coefficient of the apparatus itself may be determined by inserting a certified reference specimen, normally SRM 739, Fused Silica from the National Institute for Standards and Technology, USA or a platinum reference test-piece for high temperatures. The procedure is documented in NPL QPDMM/B120, and follows EN 821-1.

The overall accuracy of the measurement is controlled by the mechanical stability of the specimen in the apparatus. Assuming complete stability, the measurement accuracy is considered to be approximately  $\pm 0.1 \times 10^{-6} \text{ }^{\circ}\text{C}^{-1}$  in coefficient over a 100  $^{\circ}\text{C}$  temperature range or  $\pm 1\%$  in expansion, whichever is the greater.

The present tests were run at 2  $^{\circ}\text{C}/\text{min}$  to the selected maximum temperature in a flushed argon atmosphere, followed by cooling to room temperature at the same rate. At least three thermal cycles were made on each solid test-piece. A single run was made on piston dilatometer samples.

### 3.3 Piston dilatometry

The technique for piston dilatometry has been adequately described elsewhere [1, 2, 3]. Ceramic piston cells in the form of standard 4 mm bore 50 mm long liquid metering devices were fabricated by Friedrichsfeld GmbH and supplied via Degussa UK Ltd. The piston rods had been individually honed in matching cylinders to give minimal clearance, but a smooth sliding, almost frictionless fit. These units were then diamond saw cut to provide two piston cells, each with two pistons (Figure 1). The ends of the pistons were ground flat and perpendicular to the cylinder axis using the cylinder ends as a holder for the pistons.

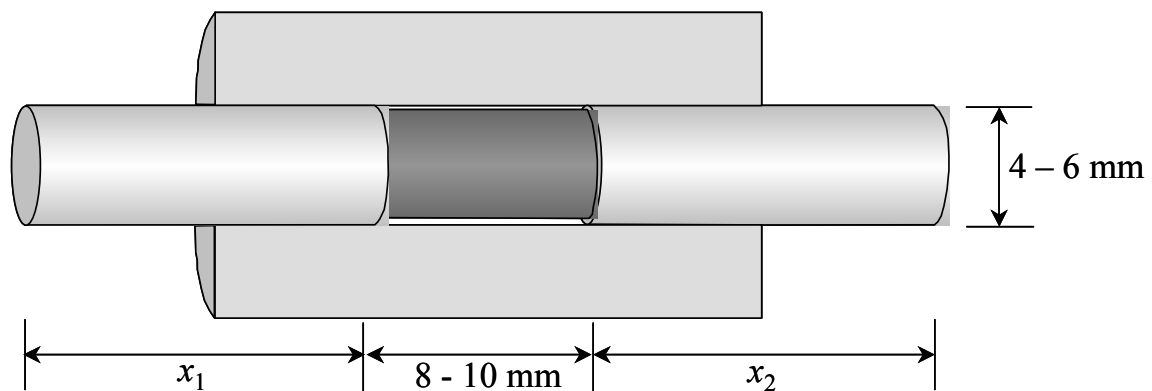


**Figure 1:** Piston cell containing a cylinder of test material.

The test material was machined to a small cylinder 8 – 10 mm in length and diameter about 1% less than the cylinder bore diameter (4.00 mm). This allows for the thermal expansion of the sample relative to the cell up to the melting point, so that there is a minimal gap at the onset of melting and no risk of breaking the cell at lower temperatures.

The test sample mass and dimensions are recorded, and it is placed in the cell, which is then treated as a solid test-piece as far as making a thermal expansion measurement is concerned. The spring force applied to the pistons is the maximum available in the dilatometer, about 3 N. The raw data recorded by the data logger are then processed as though the cell is a homogeneous sample in order to apply the dilatometer corrections for baseline shift and apparatus expansion. A typical output result is shown in Figure 2.

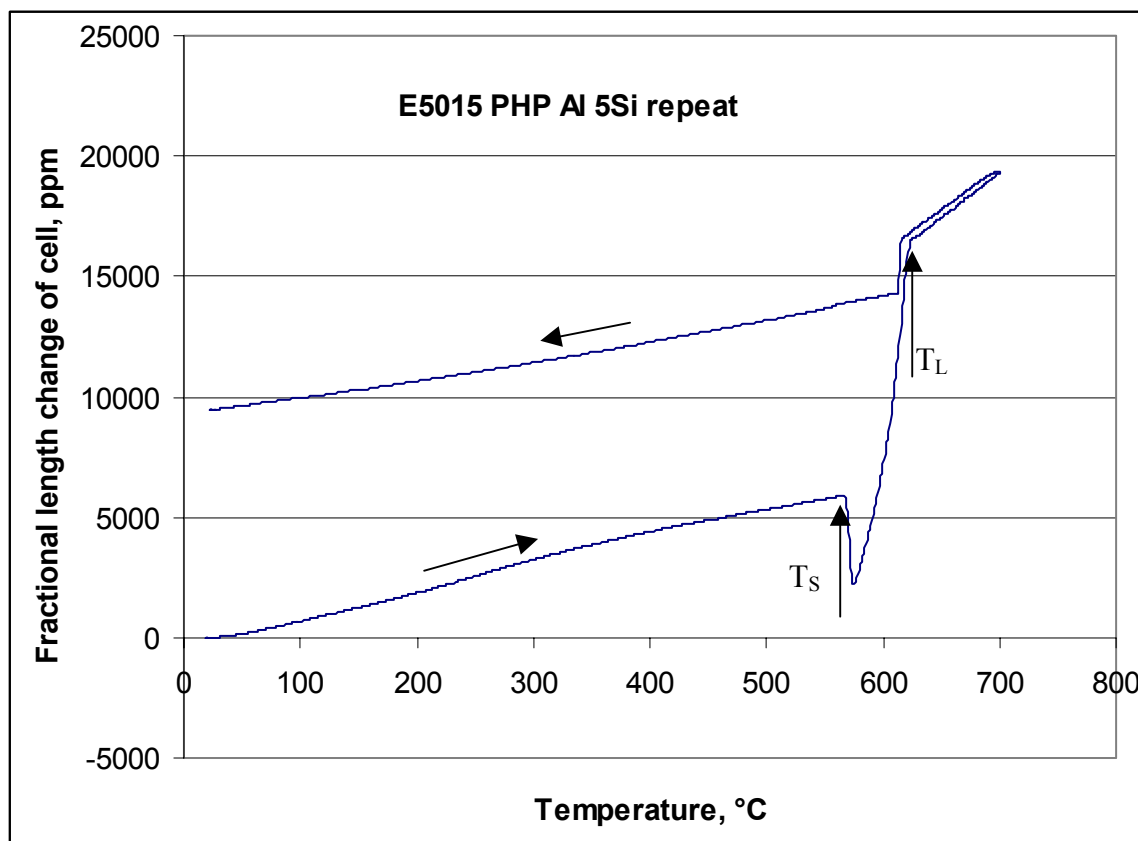


**Figure 2:** A typical example of the effective fractional length change as a function of temperature for an Al 5Si sample in a piston cell taken through the melting range and back again. At 570 °C on heating ( $T_s$ ), melting begins, and the sample collapses to fill the full diameter of the cylinder. As melting continues, the sample volume increases rapidly until melting is completed. Above the liquidus temperature ( $T_L$ ), the volumetric expansion of the liquid is recorded. On cooling, the liquid contracts and starts to solidify, but the pistons then jam and do not follow the full cooling curve.

This output then processed further in an Excel spreadsheet in three steps:

1. The expansion of the piston material determined in a separate measurement is subtracted from the total expansion to give the effective linear expansion of the alloy. Assuming the alloy has isotropic behaviour, the apparent solid density as a function of temperature up to the onset of melting can be thus be determined.

2. For temperatures above the point at which 'mush' fills the cylinder cavity, the volume of the cavity as a function of temperature is computed from the cylinder expansion behaviour and the apparent change in length of the test sample and the pistons. Assuming no liquid losses, the density of the liquid phase is computed from the starting mass of the sample and the cavity volume.
3. For temperatures above the liquidus, the fractional volume change (in practice, the fractional change in reciprocal density) is plotted as a function of temperature and a straight line fitted, the slope of which gives the volumetric expansion coefficient.

The reliability of this technique is subject to experimental factors, particularly:

1. Prediction of the solid density as a function of temperature for the sample in the cell becomes unreliable if the sample anneals or softens before melting commences. More-reliable data can usually be obtained from a larger sample tested as a conventional test-piece, rather than using the cell.
2. Any tendency for the liquid to leak small down the gap between the piston and the cylinder wall. This factor makes the cooling curves uncertain.
3. Any tendency for the solid or liquid to react with and bond to the cell wall preventing free sliding of the pistons.

In practice it has been found that the melting behaviour of aluminium and nickel alloys can be measured fairly reliably, the oxide skin helping to contain the liquid and reduce the risk of leakage. Tests on cast irons, which have high surface tension, do not suffer from leakage, but because the meniscus cannot readily be flattened in contact with the pistons, a volume error arises which is difficult to correct. In contrast, low-melting alloys which do not develop an oxide skin are prone to leakage, and give unreliable estimates of liquid volume.

The cooling data are always much less successful than the heating data for a number of reasons:

1. The duration of holding at high temperatures often means that reactions or slight leakage have occurred which cannot be overridden by push-rod force during contraction of the sample.
2. Undercooling may occur if nucleation is restricted in any way.
3. There is no means of 'feeding' the solidifying sample, which may cavitate and thus indicate an erroneous volume.

For these reasons, focus in this report is on the heating only data.

## 4. RESULTS

### 4.1 Nickel alloys, Studio programme

Of the four alloys listed in Table 1, successful runs could be made on three of them. Only with CM186LC was there a problem of leakage and welding of the pistons. A summary of the data derived is given in Table 4.

**Table 4: Results summary for nickel alloys (Studio project)**

Material	Apparent solidus temperature, °C	Apparent liquidus temperature, °C	Apparent solid density at solidus, Mg m <sup>-3</sup>	Apparent liquid density at liquidus, Mg m <sup>-3</sup>	Volumetric expansion coefficient, 10 <sup>-6</sup> °C <sup>-1</sup>
IN738LC	1300	1332	7.60	7.330	66
CMSX10	1386	1405	8.45	8.133	50
CM186LC*	1310	1340	8.18	8.147	-
René 80	1300	1320	7.55	7.359	57

\* results unreliable owing to suspected piston jamming

#### 4.2 Aluminium alloys

The experimental data for density shown in Table 5 are based on both the immersion technique and on mass and dimensions of a regular machined bar sample about 50 mm in length, 6 mm diameter. Data from literature sources are generally poor. The immersion data are plotted against silicon content in Figure 2, which shows a reasonable correlation.

**Table 5: Results summary for aluminium alloys**

Alloy composition	Density at room temperature, Mg m <sup>-3</sup>		
	Theoretical/ databook	Experimental	Experimental
		immersion	mass/dimensions
Al	2.6989	2.6885 ± 0.0016	-
Al-5Si (1)	2.69	2.6826 ± 0.0015	2.685
Al-7Si	2.67	2.6695 ± 0.0019	2.675
Al-9Si	2.67	2.6614 ± 0.0021	2.665
Al-12Si	2.66	2.6400 ± 0.0001	2.651
Al 5Si 0.3Mg	2.7	2.6715 ± 0.0006	2.682
Al 7Si 0.3Mg		2.6677 ± 0.0012	2.672
Al 9Si 0.3Mg		2.6562 ± 0.0007	2.667
Al 12Si 0.3Mg		2.6408 ± 0.0047	{2.598}*

\* Subsequently found to be cavitated

Table 6 shows a summary of the results of the piston dilatometry experiments on the alloy series and a comparison of these results with thermodynamic predictions made using the NPL Virtual Measurement System (VMS) model [4]. There is a quite reasonable match between theoretical and experimental densities of the liquid phase (Figure 3), but less good between predicted apparent solid density at the solidus, reflecting the difficulties associated with softening of the samples before the onset of melting (Figure 4). It is thought that this is due to no account being taken of the plastic collapse of the test sample close to the solidus temperature, giving an overestimate of density.

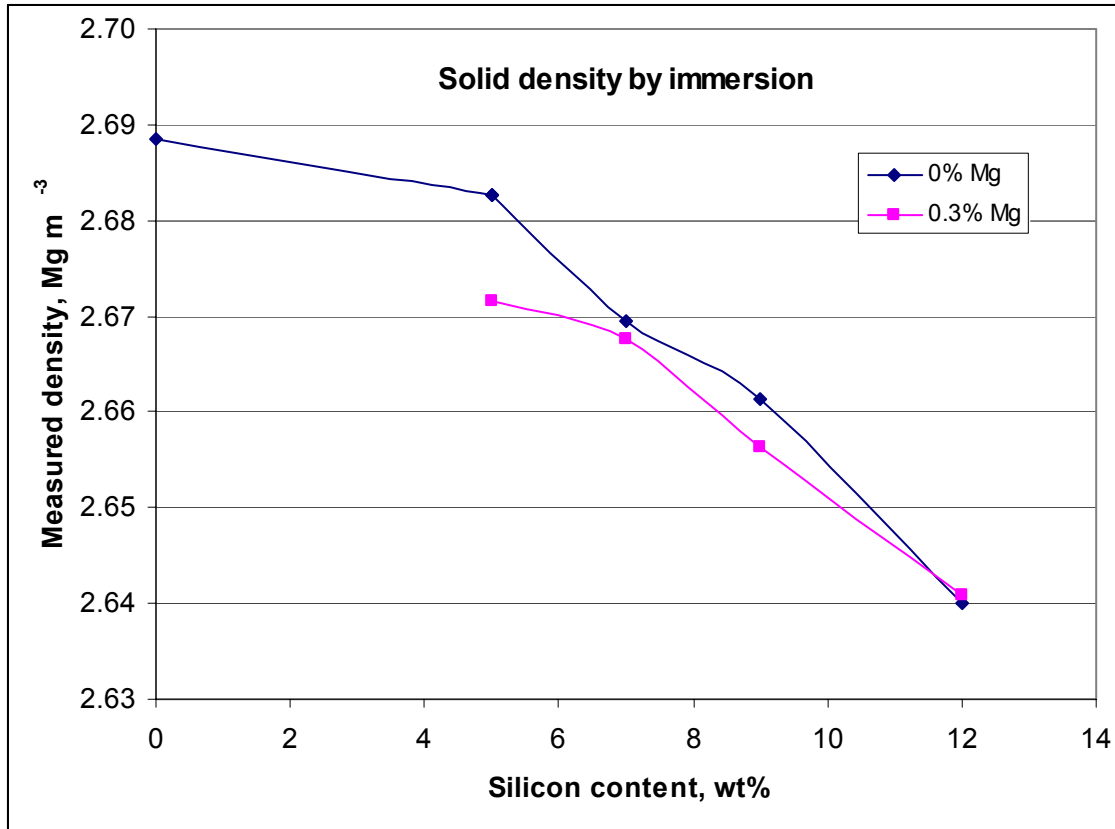


**Figure 2:** Solid density as a function of silicon content for Al-Si and Al-Si-Mg alloy series.

**Table 6: Comparison of theoretical and experimental melting parameters for aluminium alloys**

Alloy composition	Solid density at solidus, Mg m <sup>-3</sup>		Liquid density at liquidus, Mg m <sup>-3</sup>		Solidus temperature, °C		Liquidus temperature, °C		Liquid expansion coeff., 10 <sup>-6</sup> °C <sup>-1</sup>	
	Theory	Expt.	Theory	Expt.	Theory	Expt.	Theory	Expt.	Theory	Expt.
Al	2.572	2.57	2.385	2.378	660	660	660	662	118.4	122
Al-5Si (1)*	2.575	2.609	2.414	2.418	577	577	630	617	119.1	{27.3}*
Al-5Si (2)**		2.589		2.404		576		623		130
Al-7Si	2.569	2.6205	2.423	2.435	576	588	616	612	119.4	126
Al-9Si	2.563	2.592	2.433	2.418	576	574	601	602	119.7	125
Al-12Si	2.554	2.587	2.448	2.453	576	572	580	580	120.1	128
Al 5Si 0.3Mg	2.573	2.597	2.407	2.414	567	605	628	626	118.9	122
Al 7Si 0.3Mg	2.566	2.579	2.423	2.413	567	572	617	610	119.2	121
Al 9Si 0.3Mg	2.560	2.578	2.430	2.413	567	566	602	598	119.5	123
Al 12Si 0.3Mg	2.551	2.573	2.447	2.451	567	566	579	579	120.0	123

\* pistons jammed \*\* second successful run

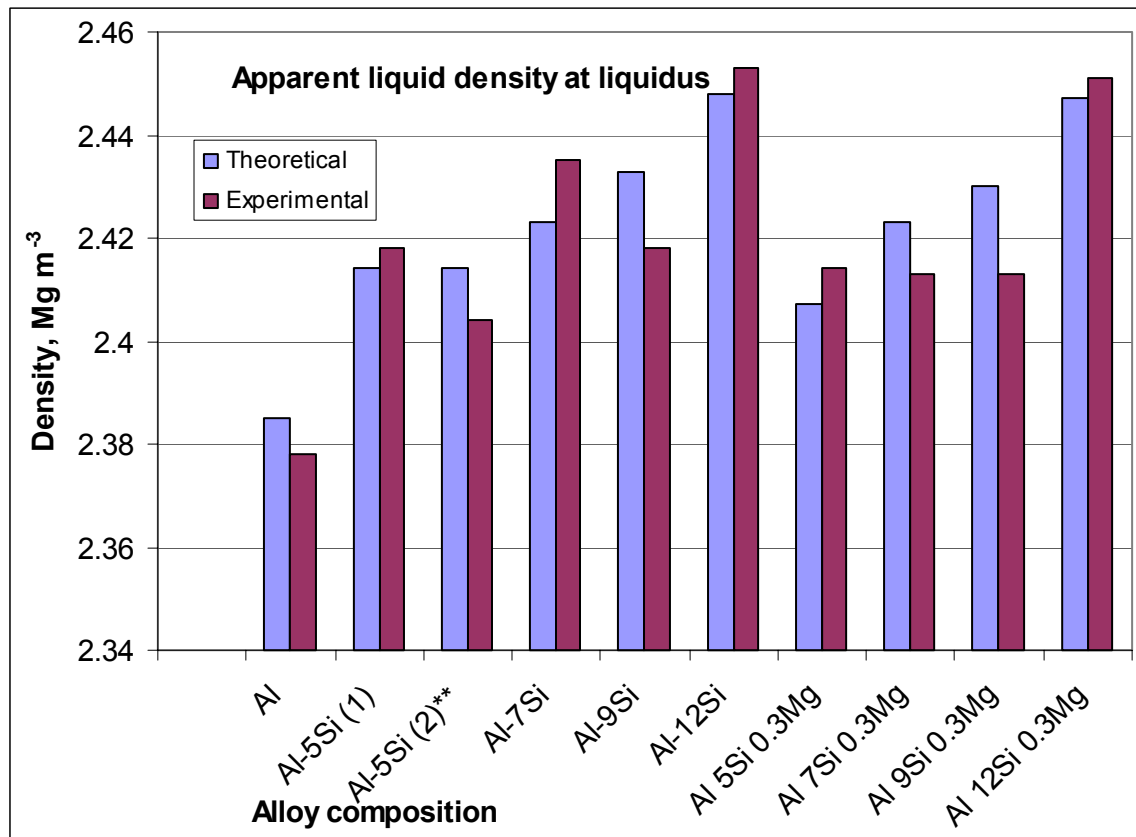


**Figure 3:** Apparent liquid density at the liquidus for the range of aluminium alloys

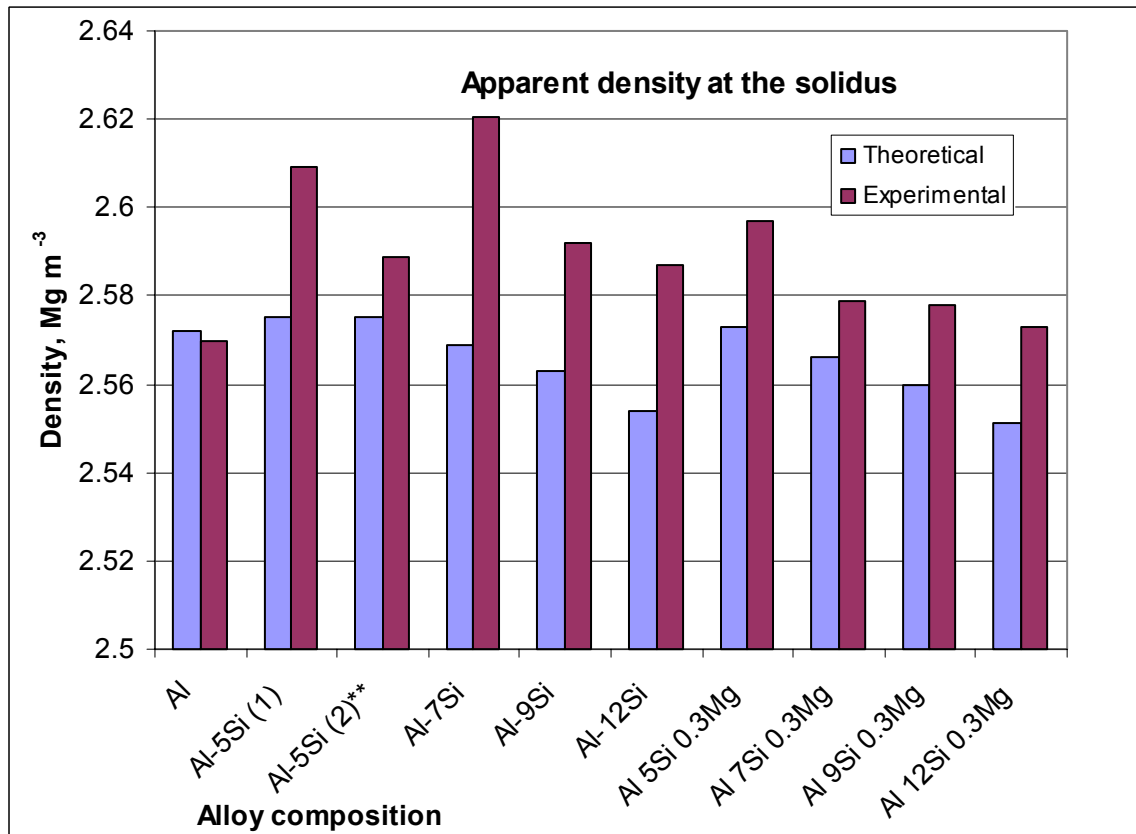


**Figure 4:** Apparent solid density at the solidus for the range of aluminium alloys.

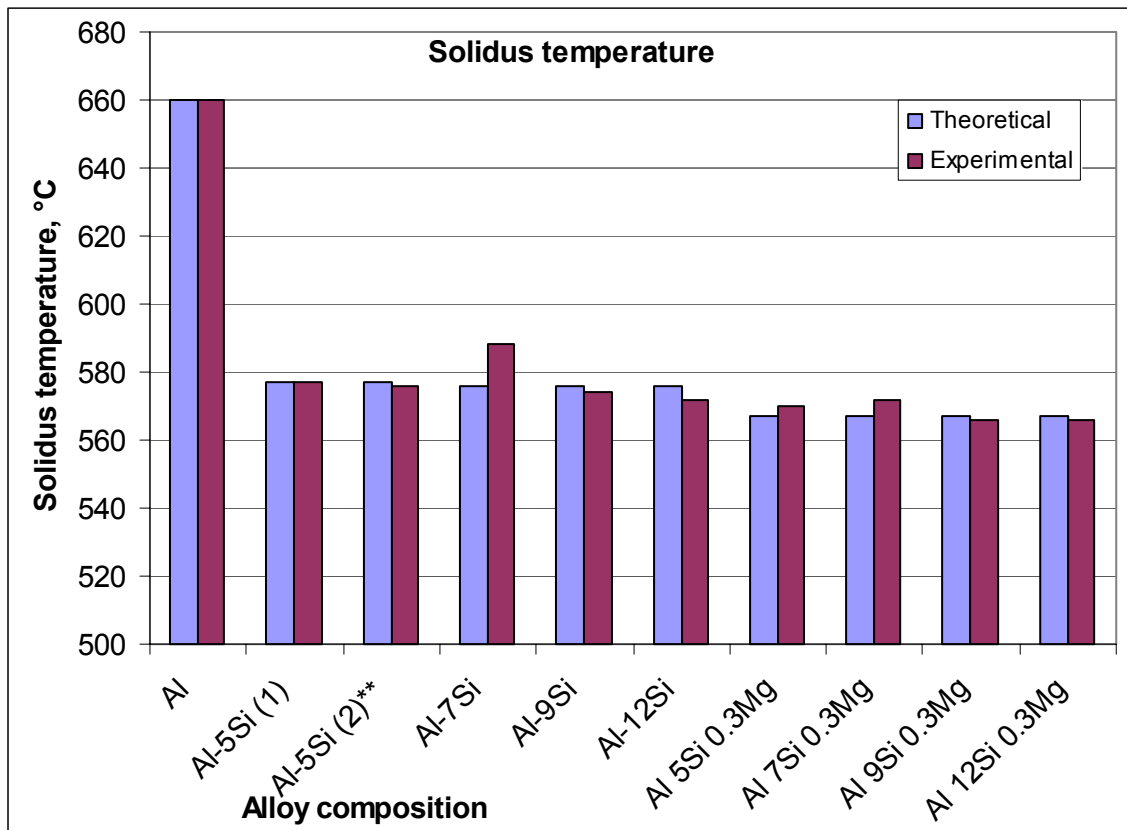


**Figure 5:** Experimentally determined solidus temperatures compared with theoretically derived ones.

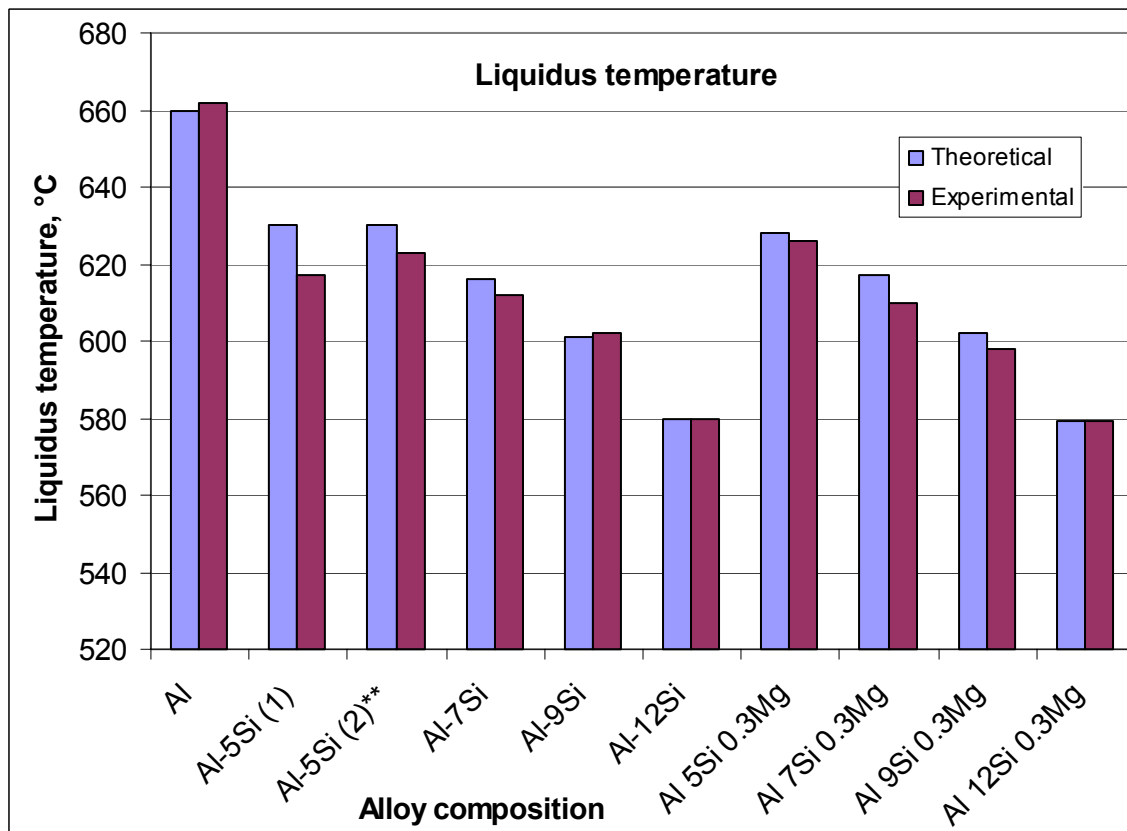


**Figure 6:** Experimentally determined liquidus temperatures compared with theoretically derived ones.

Figures 5 and 6 show good matches, usually less than 5 °C, between the solidus and liquidus temperatures determined experimentally and those determined theoretically. With particular regard to solidus temperature determination, it seems clear that this series of aluminium alloys tends to become very soft immediately the solidus temperature is achieved, and that the ‘mush’ has very little if any strength over its entire temperature range. Had there been a rigid dendritic network into the ‘mushy’ zone, this would have given a significantly raised apparent solidus temperature compared with the theoretical one.

Figure 7 shows the volumetric expansion coefficient of the liquid alloys above the liquidus determined theoretically and experimentally. Again there is quite a reasonable match, the maximum difference being 9%. Generally, a slightly higher figure is obtained experimentally than that predicted, and this could arise if the correction of the raw data for the thermal expansion coefficient of the pistons and cylinder is a little lower than the true value by as little as 3% over the temperature range involved, or by about 0.7% over the entire temperature range from room temperature. This level of error is within the typical uncertainty band of thermal expansion measurements undertaken with a mechanical dilatometer, which comprises uncertainties from temperature measurement, mechanical reproducibility and calibration errors.

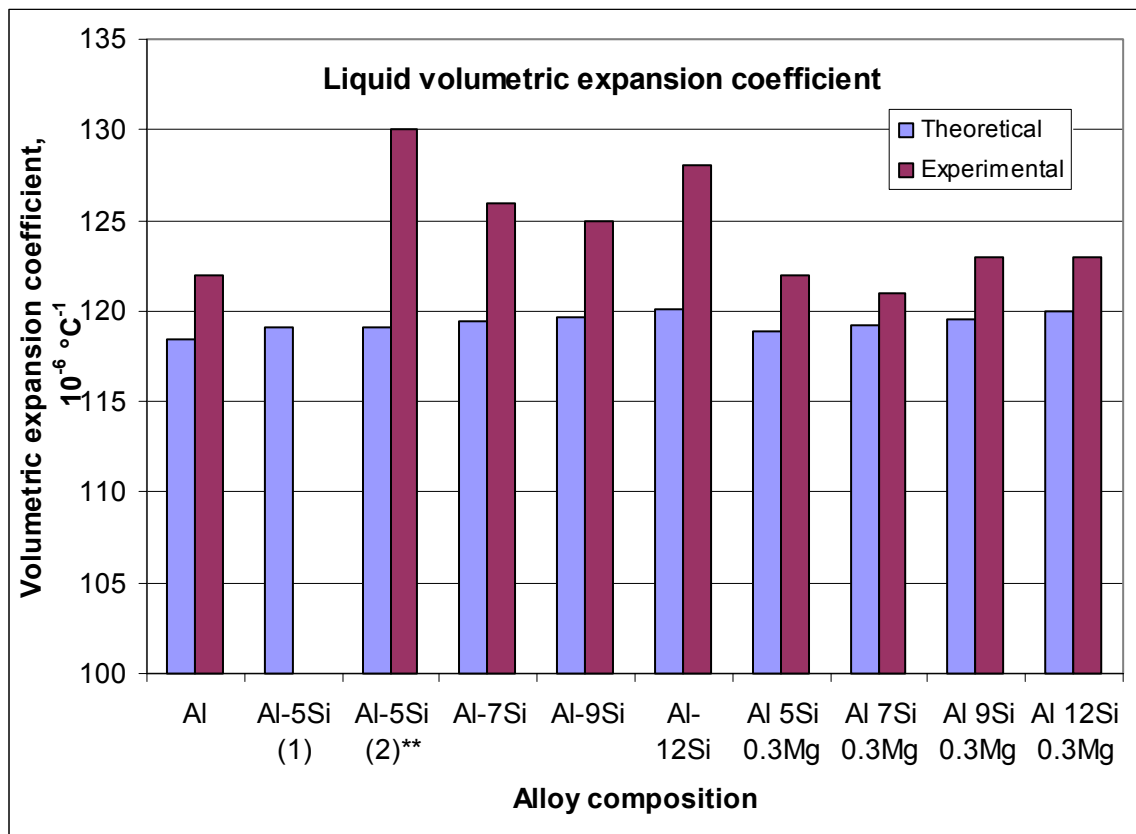


**Figure 7:** Comparison of theoretical and experimental volumetric expansion coefficients above the liquidus temperature.



### 4.3 Miscellaneous alloys

The melting curve of Waspaloy was followed readily (Figure 8), and the volumetric expansion coefficient of the liquid was determined as  $59 \times 10^{-6} \text{ }^{\circ}\text{C}^{-1}$ , a similar value to those recorded in previous work on other nickel alloys (Table 4). The melting range is described commercially as being  $1330\text{--}1360 \text{ }^{\circ}\text{C}$ <sup>1</sup>, a range which matches well with the liquidus temperature in this work of  $1355 \text{ }^{\circ}\text{C}$ .

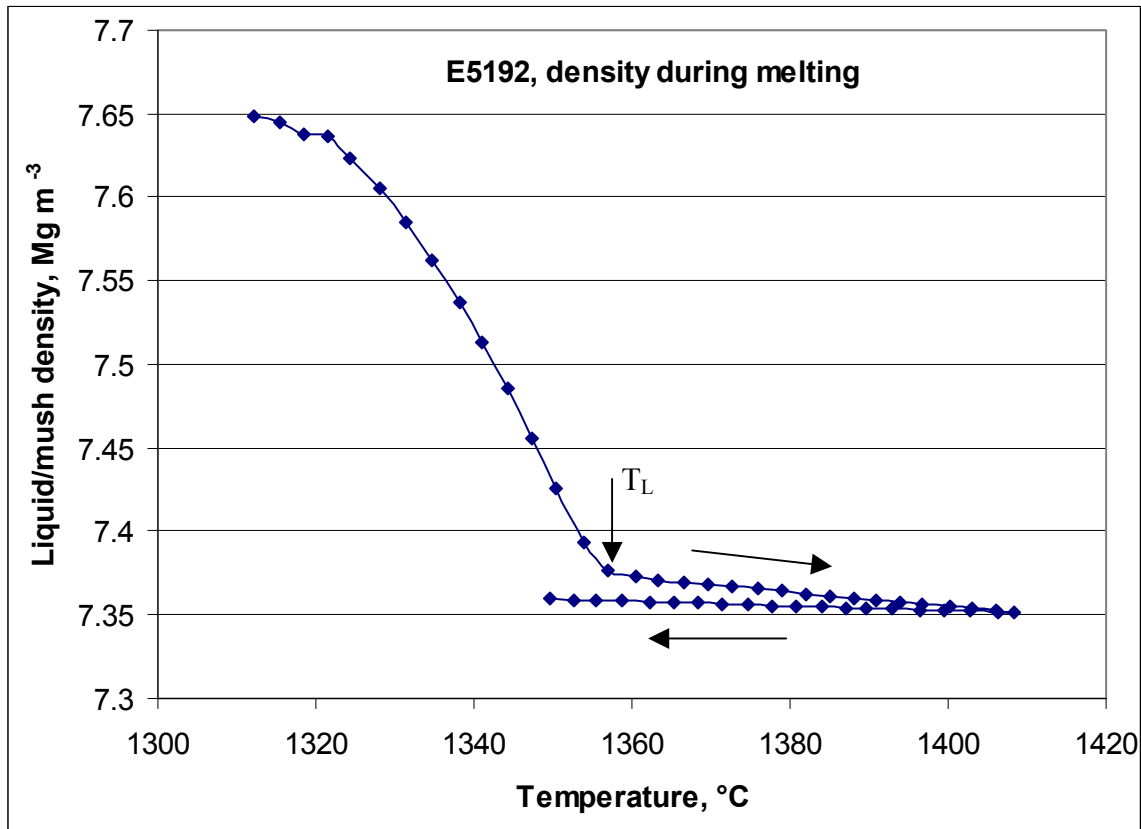


**Figure 8:** Density of Waspaloy through the ‘mush’ and into the liquid zone. The liquid cooling part of the curve indicates jammed pistons.

The melting curve of the Cu-Ni alloy (Figure 9) indicated an apparent solidus temperature of  $1175 \text{ }^{\circ}\text{C}$  and an apparent liquidus temperature of  $1223 \text{ }^{\circ}\text{C}$ . The liquid expansion coefficient between the liquidus temperature and  $1400 \text{ }^{\circ}\text{C}$  on heating was determined as  $87 \times 10^{-6} \text{ }^{\circ}\text{C}^{-1}$ , with a similar value being obtained on cooling down to  $1300 \text{ }^{\circ}\text{C}$ , indicating the achievement some element of reversible behaviour. Below this temperature, the pistons jammed. This information can be compared with the theoretical estimates made using the NPL Virtual Measurement System. Figure 9 also shows the theoretical calculations of density for a five component alloy of exactly the composition given in Table 3. The theoretical solidus is well below  $1000 \text{ }^{\circ}\text{C}$  as a consequence of a significant amount of silicon, but significant melting in a microstructural equilibrium situation starts at  $1170 \text{ }^{\circ}\text{C}$ , and the theoretical liquidus is  $1228 \text{ }^{\circ}\text{C}$ , values which are very close to the experimental ones. The theoretical volumetric expansion coefficient of the liquid above the liquidus temperature is  $104 \times 10^{-6} \text{ }^{\circ}\text{C}^{-1}$ . In contrast, the Scheil cooling model, which assumes non-equilibrium and variable composition

<sup>1</sup> <http://www.haynesintl.com/WASPALOYalloy/H3128a1.htm>

of the solidifying solid solution, does not provide as good a match, which implies that the material has achieved closed to equilibrium conditions despite the test sample being cut from a cast billet. Computations based on Cu and Ni alone indicated that the solidus temperature and melting range are very sensitive to the minor components, and their inclusion should be an essential element of any computation.

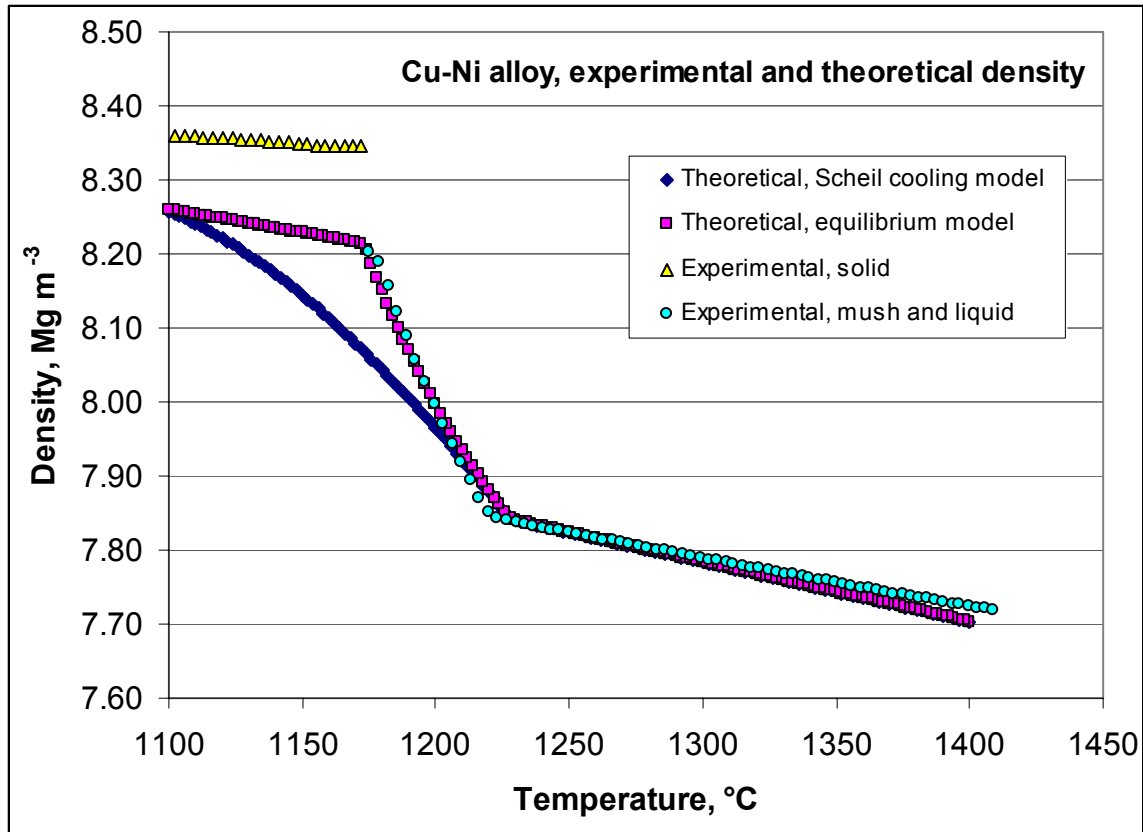


**Figure 9:** Density of Cu-Ni alloy through the ‘mushy’ zone and into the liquid, compared with theoretical predictions from the NPL Virtual Measurement System using the Scheil cooling model and the phase equilibrium model. It is clear that the material structure is in close to equilibrium conditions during the piston dilatometry experiment.

The tests on 316L stainless steel were initially unsuccessful with indistinct melting behaviour and some leakage. There appeared to have been some reaction with the piston cell walls, which turned pink from chromium diffusion. To prevent leakage, the ends of a test-piece were sprayed with boron nitride to restrict wetting, and this was reasonably successful (Figure 10). The apparent solidus temperature was determined as 1400 °C, and the liquidus was 1427 °C. The volumetric liquid expansion coefficient between the liquidus temperature and 1453 °C on heating was determined as  $58 \times 10^{-6} \text{ }^{\circ}\text{C}^{-1}$ . Some data were derived from the cooling curve, but there was significant deviation once the temperature dropped below the liquidus.

Recent measurements of electrical resistivity as a function of temperature as the through the solidus range using the ETMT<sup>2</sup> as part of the present project have suggested some liquid phase is produced at about 1375 °C, while length change measurements suggest a temperature nearer 1385 °C. Differential scanning calorimetry experiments on the same

<sup>2</sup> NPL’s Electro-Thermal Mechanical Tester, using miniature specimens

coded alloy, but from different sources and vintages suggest the onset of the melting as being at about 1385 °C [5] and 1400 °C [6], and the liquidus temperature to be about 1450 °C [5], although a source cited in [5] suggests lower temperatures, and a plot of fraction solid as a function of temperature seems to indicate a liquidus closer to 1424 °C. It therefore appears that the present piston dilatometry experiments have produced data very close to those provided by alternative techniques.

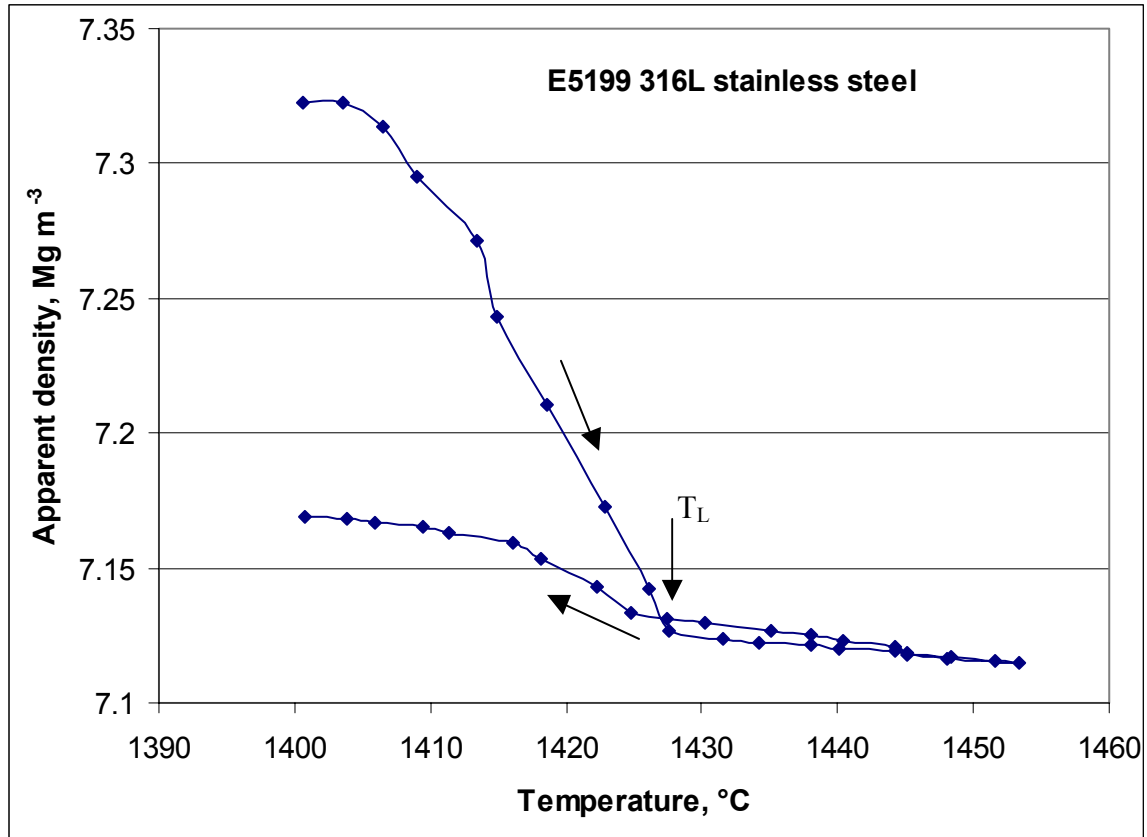


**Figure 10:** Density of 316L stainless steel through the ‘mushy’ zone and into the liquid.

## 5 DISCUSSION

The experimental results described above illustrate that the principle of piston dilatometry is sound, and works acceptably well on a range of alloy types, particularly during heating. There is a close match with the Virtual Measurement System data for solidus, liquidus and mushy zone behaviour, as well as for liquid volumetric expansion coefficient, for a range of aluminium-silicon alloys and for a copper-nickel alloy. During cooling, the system is contracting, and the force capable of being applied by the dilatometer push-rod to the pistons is limited. Any liquid leakage along the pistons, or any reaction with or deposit on the cylinder wall, will provide an obstacle to the piston, such that it no longer follows the cooling process. On occasions, where reaction is minimal, the cooling process can be followed well into the mush. A small degree of undercooling is often noted.

The cell material employed for the majority of experiments was high-purity alumina. This has the advantage of being commercially available as suitably sized piston pump components offering matched polished surfaces on pistons and cylinder bore. However, alumina can react with many molten metals at high temperatures. It has a significant vapour pressure above

1300 °C, and can diffusion bond to any oxide layer developed on the test sample. The alternative approach would be to use hot-pressed boron nitride, because of its relatively weak interaction with molten metals. However, this material, being rather soft, is much more difficult to prepare as piston cells with a reliable smooth sliding fit and minimal leakage. Any anisotropy in thermal expansion also becomes a complication of characterisation and data processing.

Success with precision-made alumina cells appears to rely on several factors:

1. Machining the diameter of the cylindrical test-piece to approximately 1-1.5% less than the internal diameter of the cylinder, so that the gap is completely taken up by differential thermal expansion by the time the solidus temperature is reached. If the test-piece is made too small, there is a sudden drop in length when the mush collapses. If its diameter is too large, there is a risk of bursting the cylinder.
2. Minimising the risk of oxidation products adhering to cylinder wall by operating in a neutral or reducing atmosphere, although as mentioned above the ability to remove all oxygen is limited by the presence of alumina itself. Some oxidation of the surface may be useful in restricting molten metal access to the gap between pistons and cylinder. A successful run on 316L stainless steel was attributed to the use of a thin boron nitride spray coating on the sample ends to separate the sample from the pistons.
3. The collapse of the test-piece immediately on reaching the solidus temperature. If a dendritic skeleton persists with significant strength into the mushy zone, it will prevent the immediate collapse, and the melting curve seen will not be the true behaviour.

Experimental experience has shown the following limitations:

1. If the machined test-piece undergoes annealing during heating with an apparent change in length (usually a reduction), or becomes soft as the solidus temperature is approached, the true expansion behaviour to the solidus temperature is not properly recorded, giving a mismatch between the computed solid density at the solidus and the trend seen at the start of the mushy zone.
2. If there is no interaction between the molten alloy sample and the cell, and the cell is apparently able to follow the cooling behaviour of the sample into the mushy zone, the final stages of solidification will usually result in void formation within the sample as a result of the usual solid phase growth mechanisms and segregation of the remaining liquid. There are very few alloys in which there is no significant shrinkage between liquid and solid. The consequence is that the solid density on cooling can be significantly underestimated. The closed volume employed by the technique offers no opportunity for 'feeding' the solidifying sample, and the force applied by the dilatometer is insufficient to deform the sample once a rigid grain network is formed.
3. Metals and alloys which have low surface tension in the molten condition, and which either do not form oxide skins or where the oxide skin is very weak, can leak out of between the cell wall and the pistons. If this occurs, the volume of the liquid is underestimated, and hence the density is overestimated. This condition can also jam

the pistons through reaction, and the apparent liquid volumetric expansion coefficient computed is then roughly three times that of the linear expansion of the cell material. An immediate indicator that this is occurring is when a low liquid volumetric expansion coefficient (less than  $30 \times 10^{-6} \text{ }^{\circ}\text{C}^{-1}$ ) is obtained. Post-mortem analysis of the sample and cell can confirm the suspicions.

## 6. CONCLUSIONS

Piston dilatometry has been applied reasonably successfully to a range of metal alloys including aluminium-silicon alloys, nickel superalloys, a copper-nickel alloy and a stainless steel. With particular regard to the aluminium alloy series, the obtained data for solidus temperature, liquidus temperature, density of the melt at the liquidus, and volumetric expansion coefficient of the liquid, match well with theoretical predictions based on thermodynamic data using NPL's MTDATA database and the recently developed Virtual Measurement System (VMS).

The technique relies on retention of the liquid metal in the confines of the cell and the occurrence of minimal reaction between the molten sample or associated oxide films and the cell wall. Provided this condition is achieved, data can be readily obtained during heating. The risks of obtaining inappropriate data are highest on cooling where the pistons fail to follow properly the contraction of the melt and then mush, but there are clear indicators when this occurs.

## ACKNOWLEDGEMENTS

This work has been supported by the Department of Trade and Industry under its Materials Metrology Programme within Project MPM6.5.

The authors would like to thank Wilfried Bender, of Hydro Aluminium Deutschland GmbH, for supplying the Al-Si alloy series as part of the MEBSP project, and Alan Dinsdale and Jim Robinson for provision of thermodynamic calculated behaviour information from the NPL Virtual Thermal System.

## REFERENCES

- [1] Morrell, R., Queded, P.N., "Evaluation of piston dilatometry for studying the melting behaviour of metals and alloys", *High Temp. - High Press.*, 2003/4, (4), 417-35.
- [2] Morrell, R., Queded, P.N., "Dilatometric measurement of melting behaviour of metal alloys", NPL Report CMMT (A) 106, 1998.
- [3] Blumm, J., Henderson, J.B., "Measurement of the volumetric expansion and bulk density of materials in the solid and molten regions", *High Temp. - High Press.*, 2000, **32**, 109-113.
- [4] Davies, R.H., Dinsdale, A.T., Gisby, J.A., Robinson, J.A.J., Martin, S.M., "MTDATA - Thermodynamics and phase equilibrium software from the National Physical Laboratory", *CALPHAD*, 2002, **26**(2), 229-271. See also: Robinson, J.A.J., Dinsdale,

- A.T., Chapman, L.A., Monaghan, B.J., Morrell, R., Quested, P.N., “The prediction of thermophysical properties for modelling solidification of metallic melts”, *Proc. 16<sup>th</sup> Eur. Thermophysical Properties Conference*, Imperial College, 2002.
- [5] Mills, K.C., “Recommended values of thermophysical properties for commercial alloys”, Woodhead Publishing, Abington, Cambridge, UK, 2002.
- [6] Roebuck, B., “Physical properties of representative engineering alloys for high rate deformation modelling”, NPL Report CMMT (A) 283, Sept. 2000.